

10 February 1999

# A partial wave analysis of the centrally produced $\pi^+\pi^-$ system in $pp$ interactions at 450 GeV/c

The WA102 Collaboration

D. Barberis<sup>4</sup>, W. Beusch<sup>4</sup>, F.G. Binon<sup>6</sup>, A.M. Blick<sup>5</sup>, F.E. Close<sup>3,4</sup>, K.M. Danielsen<sup>10</sup>, A.V. Dolgoplov<sup>5</sup>, S.V. Donskov<sup>5</sup>, B.C. Earl<sup>3</sup>, D. Evans<sup>3</sup>, B.R. French<sup>4</sup>, T. Hino<sup>11</sup>, S. Inaba<sup>8</sup>, A.V. Inyakin<sup>5</sup>, T. Ishida<sup>8</sup>, A. Jacholkowski<sup>4</sup>, T. Jacobsen<sup>10</sup>, G.T Jones<sup>3</sup>, G.V. Khaustov<sup>5</sup>, T. Kinashi<sup>12</sup>, J.B. Kinson<sup>3</sup>, A. Kirk<sup>3</sup>, W. Klempt<sup>4</sup>, V. Kolosov<sup>5</sup>, A.A. Kondashov<sup>5</sup>, A.A. Lednev<sup>5</sup>, V. Lenti<sup>4</sup>, S. Maljukov<sup>7</sup>, P. Martinengo<sup>4</sup>, I. Minashvili<sup>7</sup>, T. Nakagawa<sup>11</sup>, K.L. Norman<sup>3</sup>, J.P. Peigneux<sup>1</sup>, S.A. Polovnikov<sup>5</sup>, V.A. Polyakov<sup>5</sup>, V. Romanovsky<sup>7</sup>, H. Rotscheidt<sup>4</sup>, V. Rumyantsev<sup>7</sup>, N. Russakovich<sup>7</sup>, V.D. Samoylenko<sup>5</sup>, A. Semenov<sup>7</sup>, M. Sené<sup>4</sup>, R. Sené<sup>4</sup>, P.M. Shagin<sup>5</sup>, H. Shimizu<sup>12</sup>, A.V. Singovsky<sup>1,5</sup>, A. Sobol<sup>5</sup>, A. Solovjev<sup>7</sup>, M. Stassinaki<sup>2</sup>, J.P. Stroot<sup>6</sup>, V.P. Sugonyaev<sup>5</sup>, K. Takamatsu<sup>9</sup>, G. Tchlatchidze<sup>7</sup>, T. Tsuru<sup>8</sup>, M. Venables<sup>3</sup>, O. Villalobos Baillie<sup>3</sup>, M.F. Votruba<sup>3</sup>, Y. Yasu<sup>8</sup>.

## Abstract

A partial wave analysis of the centrally produced  $\pi^+\pi^-$  channel has been performed in  $pp$  collisions using an incident beam momentum of 450 GeV/c. An unambiguous physical solution has been found. Evidence is found for the  $f_0(980)$ ,  $f_0(1300)$ ,  $f_0(1500)$  and  $f_J(1710)$  with  $J = 0$  in the the S-wave. The  $\rho(770)$  is observed dominantly in the  $P_0^-$ -wave and the  $f_2(1270)$  is observed dominantly in the  $D_0^-$ -wave. In addition, there is evidence for a broad enhancement in the D-wave below 1 GeV.

Submitted to Physics Letters

<sup>1</sup> LAPP-IN2P3, Annecy, France.

<sup>2</sup> Athens University, Physics Department, Athens, Greece.

<sup>3</sup> School of Physics and Astronomy, University of Birmingham, Birmingham, U.K.

<sup>4</sup> CERN - European Organization for Nuclear Research, Geneva, Switzerland.

<sup>5</sup> IHEP, Protvino, Russia.

<sup>6</sup> IISN, Belgium.

<sup>7</sup> JINR, Dubna, Russia.

<sup>8</sup> High Energy Accelerator Research Organization (KEK), Tsukuba, Ibaraki 305, Japan.

<sup>9</sup> Faculty of Engineering, Miyazaki University, Miyazaki, Japan.

- <sup>10</sup> Oslo University, Oslo, Norway.
- <sup>11</sup> Faculty of Science, Tohoku University, Aoba-ku, Sendai 980, Japan.
- <sup>12</sup> Faculty of Science, Yamagata University, Yamagata 990, Japan.

Lattice gauge calculations indicate that the lowest lying glueball should be a scalar and be in the mass range 1500-1700 MeV [1]. However, after more than 20 years of searching for glueballs there is emerging evidence that a pure scalar glueball may never be observed due to the fact that its finite width means that it mixes with nearby isoscalar  $q\bar{q}$  states with  $J^{PC} = 0^{++}$  [2]. This scenario gives rise to several states whose properties are complicated and lie somewhere between conventional  $q\bar{q}$  states and glueballs. Hence a systematic study of all isoscalar  $J^{PC} = 0^{++}$  states is required. The  $\pi\pi$  system has long been a profitable place to study  $I^G J^{PC} = 0^+ 0^{++}$  states and to date very high statistics studies have been performed using  $\pi$  induced interactions [3] and  $p\bar{p}$  annihilations [4]. This paper presents a study of the  $\pi^+\pi^-$  final state formed in central  $pp$  interactions which are predicted to be a source of gluonic final states via double Pomeron exchange [5].

The reaction

$$pp \rightarrow p_f(\pi^+\pi^-)p_s \quad (1)$$

has been studied at 450 GeV/c. The subscripts  $f$  and  $s$  indicate the fastest and slowest particles in the laboratory respectively. The WA102 experiment has been performed using the CERN Omega Spectrometer, the layout of which is described in ref. [6]. Reaction (1) has been isolated from the sample of events having four outgoing charged tracks, by first imposing the following cuts on the components of the missing momentum:  $|\text{missing } P_x| < 14.0 \text{ GeV}/c$ ,  $|\text{missing } P_y| < 0.16 \text{ GeV}/c$  and  $|\text{missing } P_z| < 0.08 \text{ GeV}/c$ , where the  $x$  axis is along the beam direction. A correlation between pulse-height and momentum obtained from a system of scintillation counters was used to ensure that the slow particle was a proton.

The method of Ehrlich et al. [7], has been used to compute the mass squared of the two centrally produced particles assuming them to have equal mass. The resulting distribution is shown in fig. 1a) where a clear peak can be seen at the pion mass squared. A cut on the Ehrlich mass squared of  $-0.3 \leq M_X^2 \leq 0.2 \text{ GeV}^2$  has been used to select a sample of 5.15 million  $\pi^+\pi^-$  events.

Fig. 1b) shows the  $p_f\pi^+$  effective mass spectrum where a clear  $\Delta^{++}(1232)$  can be observed. A smaller  $\Delta^0(1232)$  signal can be seen in the  $p_f\pi^-$  effective mass spectrum shown in fig. 1c). The  $\Delta(1232)$  signal has been removed by requiring  $M(p_f\pi) > 1.5 \text{ GeV}$ . Due to the trigger requirements there is little evidence for  $\Delta$  production in the  $p_s\pi$  effective mass spectra (not shown). However, for symmetry purposes a cut of  $M(p_s\pi) > 1.5 \text{ GeV}$  has also been applied.

As can be seen from fig. 1b) there is also some evidence for higher mass  $\Delta^{++}$  or  $N^*$  production. In order to investigate the effect of this on the following results an analysis has also been performed requiring that  $M(p\pi) > 2.0 \text{ GeV}$ . It is found that the higher mass proton excitations do not significantly influence the results.

The Feynman  $x_F$  distributions for the slow particle, the  $\pi^+\pi^-$  system and the fast particle are shown in fig. 1d). As can be seen the  $\pi^+\pi^-$  system lies within  $|x_F| \leq 0.25$ .

The resulting centrally produced  $\pi^+\pi^-$  effective mass distribution is shown in fig. 1e) and consists of 2.87 million events. As can be seen there is evidence for a small  $\rho^0(770)$  signal, some  $f_2(1270)$  and a sharp drop at 1 GeV which has been interpreted as being due to the interference of the  $f_0(980)$  with the S-wave background [8].

A Partial Wave Analysis (PWA) of the centrally produced  $\pi^+\pi^-$  system has been performed

assuming the  $\pi^+\pi^-$  system is produced by the collision of two particles (referred to as exchanged particles) emitted by the scattered protons. The  $z$  axis is defined by the momentum vector of the exchanged particle with the greatest four-momentum transferred in the  $\pi^+\pi^-$  centre of mass. The  $y$  axis is defined by the cross product of the two exchanged particles in the  $pp$  centre of mass. The two variables needed to specify the decay process were taken as the polar and azimuthal angles ( $\theta, \phi$ ) of the  $\pi^-$  in the  $\pi^+\pi^-$  centre of mass relative to the coordinate system described above.

The acceptance corrected moments, defined by

$$I(\Omega) = \sum_L t_{L0} Y_L^0(\Omega) + 2 \sum_{L,M>0} t_{LM} \text{Re}\{Y_L^M(\Omega)\} \quad (2)$$

have been rescaled to the total number of observed events and are shown in fig. 2. As can be seen the moments with  $M > 2$  and  $L > 4$  are small (i.e.  $t_{43}, t_{44}, t_{50}$  and  $t_{60}$ ) and hence only S, P, and D waves with  $m \leq 1$  have been included in the PWA.

An interesting feature of the moments is the presence of a structure in the  $L = 4$  moments for  $\pi^+\pi^-$  masses below 1 GeV which indicates the presence of D-wave. This type of structure has not been observed in  $\pi$  induced reactions [3]. In order to see if this effect is due to acceptance problems or problems due to non-central events, we have reanalysed the data using a series of different cuts. Firstly, we required that  $M(p\pi) > 2.0$  GeV; however, after acceptance correction the moments were compatible with the set for  $M(p\pi) > 1.5$  GeV showing that diffractive resonances in the range  $1.5 < M(p\pi) < 2.0$  GeV have a negligible effect on the moments. We have also required that the rapidity gap between any proton and  $\pi$  in the event is greater than 2 units. Again the resulting acceptance corrected moments do not change. In order to investigate any systematic effects we have also analysed the central  $\pi^0\pi^0$  data and a similar structure is also found in the  $L = 4$  moments [9].

It is interesting to compare the above result with previously published data on other centrally produced  $\pi\pi$  systems. In preliminary results from the E690 experiment at Fermilab activity at a similar level is observed in the  $t_{40}$  moment below 1 GeV [10]. There is also evidence for this structure in the  $\pi^0\pi^0$  data from the NA12/2 experiment [11]. The AFS experiment at the CERN ISR also observed that the  $t_{40}$  moments deviated from zero in this mass region; however, in their analysis they claimed this deviation was due to problems of the Monte Carlo simulating low energy tracks [12].

This structure does indeed seem to be a real effect which is present in centrally produced  $\pi\pi$  systems. It has recently been suggested [13, 14] that central production may be due to the fusion of two vector particles and this may explain why higher angular momentum systems can be produced at lower masses.

The amplitudes used for the PWA are defined in the reflectivity basis [15]. In this basis the angular distribution is given by a sum of two non-interfering terms corresponding to negative and positive values of reflectivity. The waves used were of the form  $J_m^\epsilon$  with  $J = \text{S, P and D}$ ,  $m = 0, 1$  and reflectivity  $\epsilon = \pm 1$ . The expressions relating the moments ( $t_{LM}$ ) and the waves ( $J_m^\epsilon$ ) are given in table 1. Since the overall phase for each reflectivity is indeterminate, one wave in each reflectivity can be set to be real ( $S_0^-$  and  $P_1^+$  for example) and hence two phases can be set to zero ( $\phi_{S_0^-}$  and  $\phi_{P_1^+}$  have been chosen). This results in 12 parameters to be determined from the fit to the angular distributions.

The PWA has been performed independently in 20 MeV intervals of the  $\pi^+\pi^-$  mass spectrum. In each mass an event-by-event maximum likelihood method has been used. The function

$$F = - \sum_{i=1}^N \ln\{I(\Omega)\} + \sum_{L,M} t_{LM}\epsilon_{LM} \quad (3)$$

has been minimised, where N is the number of events in a given mass bin,  $\epsilon_{LM}$  are the efficiency corrections calculated in the centre of the bin and  $t_{LM}$  are the moments of the angular distribution. The moments calculated from the partial amplitudes are shown superimposed on the experimental moments in fig 2. As can be seen the results of the fit well reproduce the experimental moments.

The system of equations which express the moments via the partial wave amplitudes is non-linear that leads to inherent ambiguities. For a system with S, P and D waves there are eight solutions for each mass bin. In each mass bin one of these solutions is found from the fit to the experimental angular distributions while the other seven can then be calculated by the method described in ref. [15]. In order to link the solutions in adjacent mass bins, the real and imaginary parts of the Barrelet function roots are required to be step-wise continuous and have finite derivatives as a function of mass [16]. By definition, all the solutions give identical moments and identical values of the likelihood. The only way to differentiate between the solutions, if different, is to apply some external physical test, such as requiring that at threshold that the S-wave is the dominant wave.

The four complex roots,  $Z_i$ , after the linking procedure are shown in fig. 3. As can be seen the real parts are well separated and hence it is possible to identify unambiguously all the PWA solutions in the whole mass range. In addition, the zeros do not cross the real axis and hence there is no problem with bifurcation of the solutions. Near threshold the P-wave is the dominant contribution for five solutions, another one is dominated by D-wave and another has the same amount of S-wave and P-wave. These seven solutions have been ruled out because the  $\pi^+\pi^-$  cross section near threshold has been assumed to be dominated by S-wave. The remaining solution is shown in fig. 4.

The S-wave spectrum shows a clear threshold enhancement followed by a sharp drop at 1 GeV. There is clear evidence for the  $\rho(770)$  in the  $P_0^-$  wave and for the  $f_2(1270)$  in the  $D_0^-$  wave.

In order to obtain a satisfactory fit to the  $S_0^-$  wave from threshold to 2 GeV it has been found to be necessary to use three interfering Breit-Wigners to describe the  $f_0(980)$ ,  $f_0(1300)$  and  $f_0(1500)$  and a background of the form  $a(m - m_{th})^b \exp(-cm - dm^2)$ , where  $m$  is the  $\pi^+\pi^-$  mass,  $m_{th}$  is the  $\pi^+\pi^-$  threshold mass and a, b, c, d are fit parameters. The Breit-Wigners have been convoluted with a Gaussian to account for the experimental mass resolution ( $\sigma = 4$  MeV at threshold rising to 22 MeV at 2 GeV). The fit is shown in fig. 3c) for the entire mass range and in fig. 3d) for masses above 1 GeV. The resulting parameters are

$$\begin{array}{llll} f_0(980) & M & = & 982 \pm 3 \quad \text{MeV}, & \Gamma & = & 80 \pm 10 \quad \text{MeV} \\ f_0(1300) & M & = & 1308 \pm 10 \quad \text{MeV}, & \Gamma & = & 222 \pm 20 \quad \text{MeV} \\ f_0(1500) & M & = & 1502 \pm 10 \quad \text{MeV}, & \Gamma & = & 131 \pm 15 \quad \text{MeV} \end{array}$$

which are consistent with the PDG [17] values for these resonances. As can be seen, the fit describes the data well for masses below 1 GeV. It was not possible to describe the data above

1 GeV without the addition of both the  $f_0(1300)$  and  $f_0(1500)$  resonances. However, even with this fit using three Breit-Wigners it can be seen that the fit does not describe well the 1.7 GeV region. This could be due to a  $\pi^+\pi^-$  decay mode of the  $f_J(1710)$  with  $J = 0$ . Including a fourth Breit-Wigner in this mass region decreases the  $\chi^2$  from 256 to 203 and yields

$$f_J(1710) \quad M = 1750 \pm 20 \quad \text{MeV}, \quad \Gamma = 160 \pm 30 \quad \text{MeV}.$$

parameters which are consistent with the PDG [17] values for the  $f_J(1710)$ . The fit is shown in fig. 3e) for masses above 1 GeV.

In conclusion, a partial wave analysis of a high statistics sample of centrally produced  $\pi^+\pi^-$  events has been performed. An unambiguous physical solution has been found. The S-wave is found to dominate the mass spectrum and is composed of a broad enhancement at threshold, a sharp drop at 1 GeV due to the interference between the  $f_0(980)$  and the S-wave background, the  $f_0(1300)$ , the  $f_0(1500)$  and the  $f_J(1710)$  with  $J = 0$ . The  $\rho(770)$  is observed dominantly in the  $P_0^-$ -wave. The D-wave shows evidence for the  $f_2(1270)$  and a broad enhancement below 1 GeV. It is interesting to note that the  $f_2(1270)$  is produced dominantly with  $m = 0$ . There is no evidence for any significant structure in the D-wave above the  $f_2(1270)$  i.e. no evidence for a  $J = 2$  component of the  $f_J(1710)$ .

### Acknowledgements

This work is supported, in part, by grants from the British Particle Physics and Astronomy Research Council, the British Royal Society, the Ministry of Education, Science, Sports and Culture of Japan (grants no. 04044159 and 07044098), the Programme International de Co-operation Scientifique (grant no. 576) and the Russian Foundation for Basic Research (grants 96-15-96633 and 98-02-22032).

## References

- [1] G. Bali *et al.*, Phys. Lett. **B309** (1993) 378;  
D. Weingarten, hep-lat/9608070;  
J. Sexton *et al.*, Phys. Rev. Lett. **75** (1995) 4563;  
F.E. Close and M.J. Teper, “On the lightest Scalar Glueball” Rutherford Appleton Laboratory report no. RAL-96-040; Oxford University report no. OUTP-96-35P
- [2] C. Amsler and F.E. Close Phys. Lett. **B353** (1995) 385;  
F.E. Close, G.R. Farrar and Z. Li, Phys. Rev. **D55** (1997) 5749.
- [3] B. Hyams *et al.*, Nucl. Phys. **B64** (1973) 134;  
G. Grayer *et al.*, Nucl. Phys. **B75** (1974) 189.
- [4] C. Amsler *et al.*, Phys. Lett. **B355** (1995) 425.
- [5] D. Robson, Nucl. Phys. **B130** (1977) 328;  
F.E. Close, Rep. Prog. Phys. **51** (1988) 833.
- [6] D. Barberis *et al.*, Phys. Lett. **B397** (1997) 339.
- [7] R. Ehrlich *et al.*, Phys. Rev. Lett. **20** (1968) 686.
- [8] T.A. Armstrong *et al.*, Zeit. Phys. **C51** (1991) 351.
- [9] D. Barberis *et al.*, In preparation.
- [10] M.C. Berrisso *et al.*, Proceedings of Hadron 97, AIP conf. proc. 432 (1997) 36.
- [11] D. Alde *et al.*, In preparation.
- [12] T. Åkesson *et al.*, Nucl. Phys. **B264** (1986) 154.
- [13] F.E. Close, Phys. Lett. **B419** (1998) 387;  
F.E. Close and G. Schuler, hep-ph/9802243.
- [14] P. Castoldi, R. Escribano and J.-M. Frere, Phys. Lett. **B425** (1998) 359.
- [15] S.U. Chung, Phys. Rev. **D56** (1997) 7299.
- [16] D. Alde *et al.*, Europ. Phys. Journal. **A3** (1998) 361.
- [17] Particle Data Group, European Physical Journal **C3** (1998) 1.

Table 1: The moments of the angular distribution expressed in terms of the partial waves.

$$\begin{aligned}
\sqrt{4\pi}t_{00} &= |S_0^-|^2 + |P_0^-|^2 + |P_1^-|^2 + |P_1^+|^2 + |D_0^-|^2 + |D_1^-|^2 + |D_1^+|^2 \\
\sqrt{4\pi}t_{10} &= 2|S_0^-||P_0^-|\cos(\phi_{S_0^-} - \phi_{P_0^-}) + \frac{4}{\sqrt{5}}|P_0^-||D_0^-|\cos(\phi_{P_0^-} - \phi_{D_0^-}) \\
&\quad + \frac{2\sqrt{3}}{\sqrt{5}}\{|P_1^-||D_1^-|\cos(\phi_{P_1^-} - \phi_{D_1^-}) + |P_1^+||D_1^+|\cos(\phi_{P_1^+} - \phi_{D_1^+})\} \\
\sqrt{4\pi}t_{11} &= \sqrt{2}|S_0^-||P_1^-|\cos(\phi_{S_0^-} - \phi_{P_1^-}) - \frac{\sqrt{2}}{\sqrt{5}}|P_1^-||D_0^-|\cos(\phi_{P_1^-} - \phi_{D_0^-}) \\
&\quad + \frac{\sqrt{6}}{\sqrt{5}}|P_0^-||D_1^-|\cos(\phi_{P_0^-} - \phi_{D_1^-}) \\
\sqrt{4\pi}t_{20} &= \frac{2}{\sqrt{5}}|P_0^-|^2 - \frac{1}{\sqrt{5}}(|P_1^-|^2 + |P_1^+|^2) + \frac{\sqrt{5}}{7}(2|D_0^-|^2 + |D_1^-|^2 + |D_1^+|^2) \\
&\quad + 2|S_0^-||D_0^-|\cos(\phi_{S_0^-} - \phi_{D_0^-}) \\
\sqrt{4\pi}t_{21} &= \frac{\sqrt{6}}{\sqrt{5}}|P_1^-||P_0^-|\cos(\phi_{P_1^-} - \phi_{P_0^-}) + \frac{\sqrt{10}}{7}|D_1^-||D_0^-|\cos(\phi_{D_1^-} - \phi_{D_0^-}) \\
&\quad + \sqrt{2}|S_0^-||D_1^-|\cos(\phi_{S_0^-} - \phi_{D_1^-}) \\
\sqrt{4\pi}t_{22} &= \frac{\sqrt{3}}{\sqrt{10}}(|P_1^-|^2 - |P_1^+|^2) + \frac{\sqrt{15}}{7\sqrt{2}}(|D_1^-|^2 - |D_1^+|^2) \\
\sqrt{4\pi}t_{30} &= -\frac{6}{\sqrt{35}}\{|P_1^-||D_1^-|\cos(\phi_{P_1^-} - \phi_{D_1^-}) + |P_1^+||D_1^+|\cos(\phi_{P_1^+} - \phi_{D_1^+})\} \\
&\quad + \frac{6\sqrt{3}}{\sqrt{35}}|P_0^-||D_0^-|\cos(\phi_{P_0^-} - \phi_{D_0^-}) \\
\sqrt{4\pi}t_{31} &= \frac{6}{\sqrt{35}}|P_1^-||D_0^-|\cos(\phi_{P_1^-} - \phi_{D_0^-}) + \frac{4\sqrt{3}}{\sqrt{35}}|P_0^-||D_1^-|\cos(\phi_{P_0^-} - \phi_{D_1^-}) \\
\sqrt{4\pi}t_{32} &= \frac{\sqrt{6}}{\sqrt{7}}\{|P_1^-||D_1^-|\cos(\phi_{P_1^-} - \phi_{D_1^-}) - |P_1^+||D_1^+|\cos(\phi_{P_1^+} - \phi_{D_1^+})\} \\
\sqrt{4\pi}t_{40} &= \frac{6}{7}|D_0^-|^2 - \frac{4}{7}(|D_1^-|^2 + |D_1^+|^2) \\
\sqrt{4\pi}t_{41} &= \frac{2\sqrt{15}}{7}|D_0^-||D_1^-|\cos(\phi_{D_0^-} - \phi_{D_1^-}) \\
\sqrt{4\pi}t_{42} &= \frac{\sqrt{10}}{7}(|D_1^-|^2 - |D_1^+|^2)
\end{aligned}$$



## Figures

Figure 1: a) The Ehrlich mass squared distribution, b) the  $M(p_f\pi^+)$  and c) the  $M(p_f\pi^-)$  mass spectra. d) The  $x_F$  distribution for the slow particle, the  $\pi^+\pi^-$  system and the fast particle. e) The centrally produced  $\pi^+\pi^-$  effective mass spectrum.

Figure 2: The  $\sqrt{4\pi}t_{LM}$  moments from the data. Superimposed as a solid histogram are the resulting moments calculated from the PWA of the  $\pi^+\pi^-$  final state.

Figure 3: a) The Real and b) Imaginary parts of the roots (see text) as a function of mass obtained from the PWA. c) and d) The  $\pi^+\pi^- S_0^-$  wave with fit described in the text using three Breit-Wigners. e) The  $\pi^+\pi^- S_0^-$  wave with fit described in the text using four Breit-Wigners.

Figure 4: The physical solution from the PWA of the  $\pi^+\pi^-$  final state.

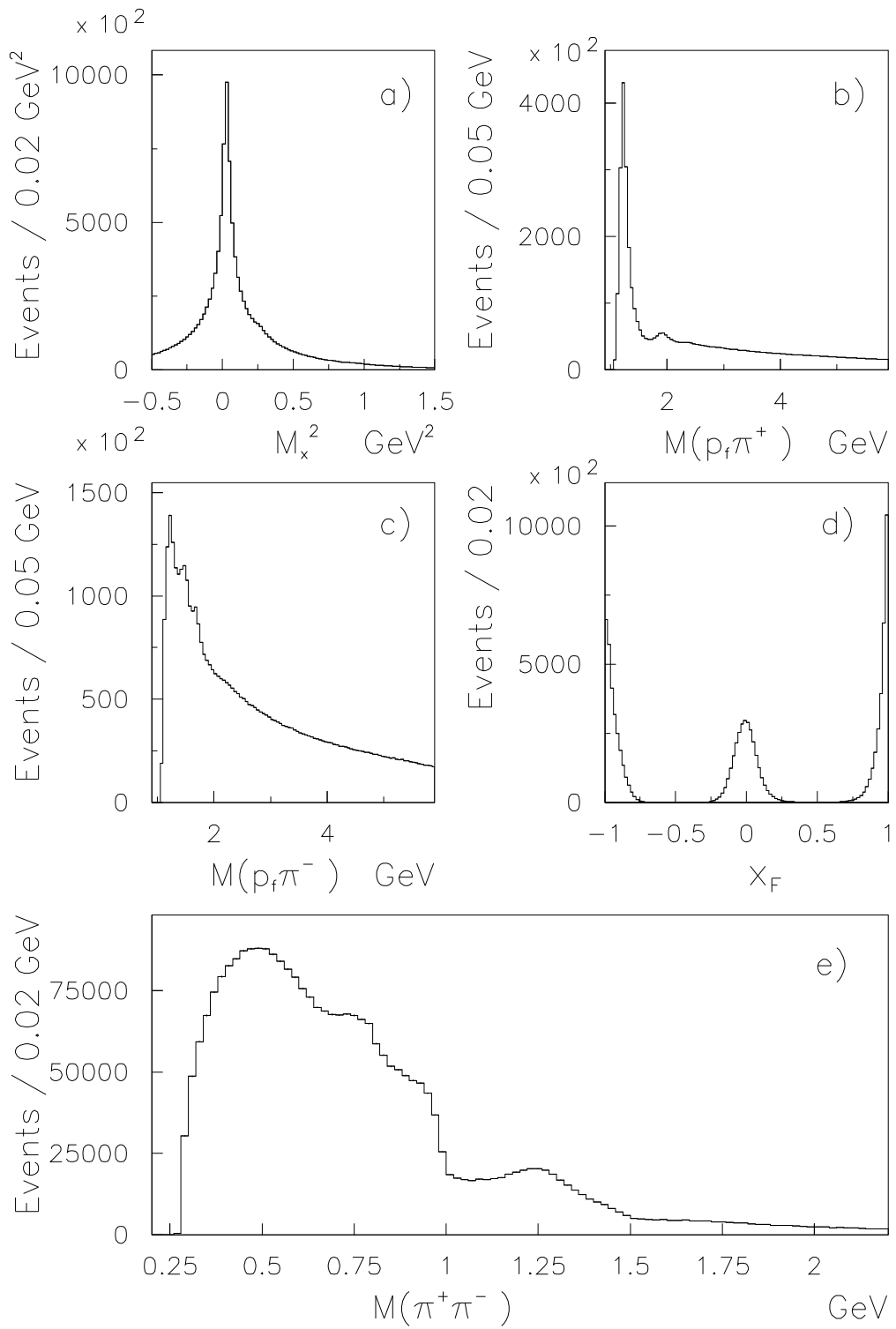


Figure 1

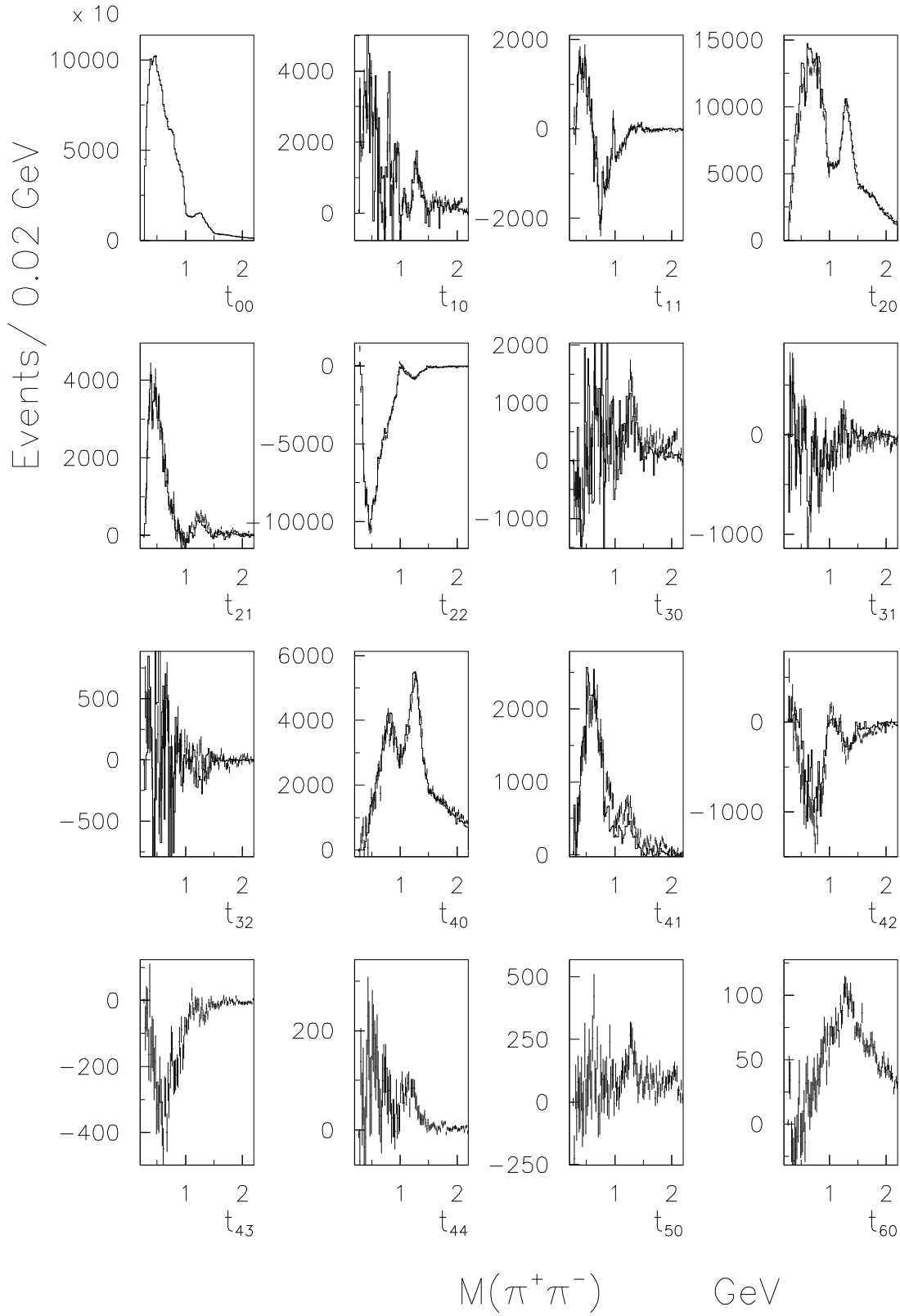


Figure 2

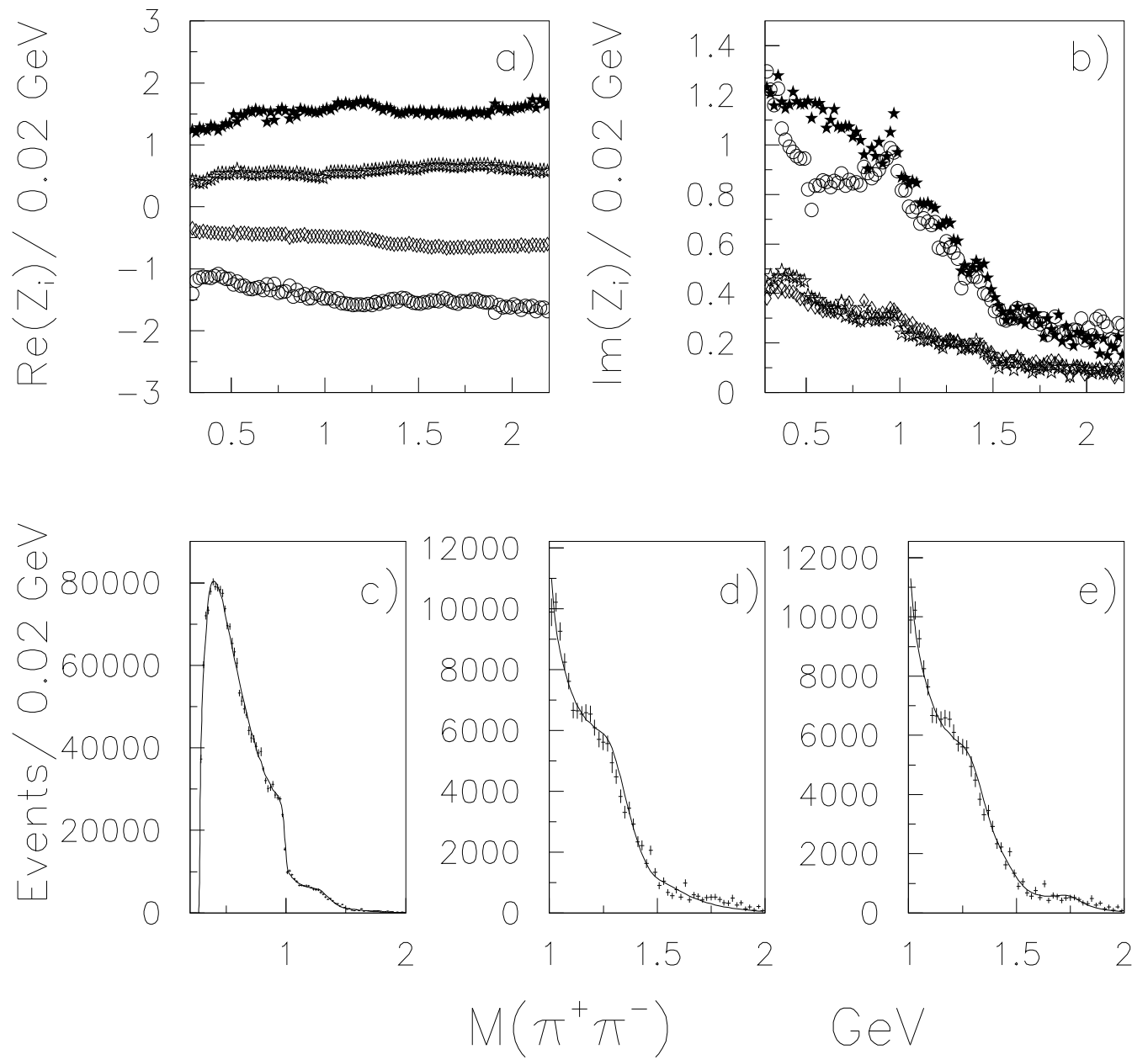


Figure 3

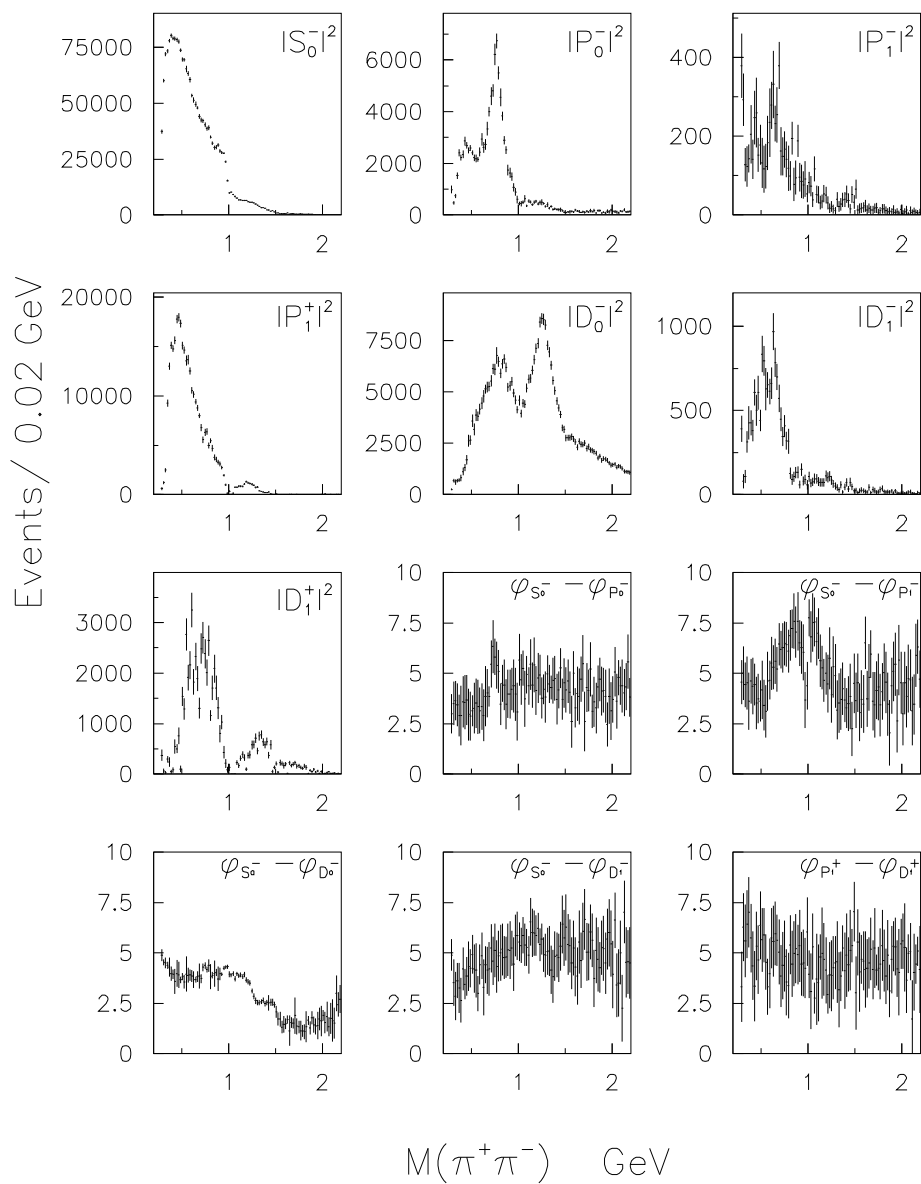


Figure 4